

## Preparation of Cobalt/Coal–Based Activated Carbon Composites with Synergistic Electrochemical Performance

Junsheng Zhu<sup>1,\*</sup>, Xu Zhang<sup>1</sup>, Shuangquan Zhang<sup>1</sup>, Dianlong Wang<sup>2</sup>

<sup>1</sup> School of Chemical Engineering and Technology, China University of Mining and Technology, Xuzhou 221116, China

<sup>2</sup> School of Chemical Engineering and Technology, Harbin Institute of Technology, Harbin 150001, China

\*E-mail: [zhujschina@163.com](mailto:zhujschina@163.com)

*Received:* 23 February 2017 / *Accepted:* 16 March 2017 / *Published:* 12 April 2017

---

A facile precipitation approach has been developed to prepare cobalt/coal–based activated carbon composites as an electrode material for supercapacitors. The existence of coal–based activated carbon facilitates the dispersion of Co particles. The electrochemical performance of Co/coal–based activated carbon composites had been characterized by cyclic voltammetry, galvanostatic charge/discharge tests and electrochemical impedance spectroscopy. The specific capacitance of the as–prepared composite material approaches  $615 \text{ F g}^{-1}$  at a current density of  $2 \text{ A g}^{-1}$ . And the composite electrode delivers an excellent rate capacity of  $495 \text{ F g}^{-1}$  even at a current density as high as  $20 \text{ A g}^{-1}$ . The impressive performance could be ascribed to the synergistic effect of the combination of the pseudocapacitive cobalt nanoparticles and the coal–based activated carbon matrix.

---

**Keywords:** Cobalt; Coal–based activated carbon; Supercapacitors; Composites

### 1. INTRODUCTION

Supercapacitors, as excellent electrochemical power sources, have attracted intensive attention due to their high charge/discharge rate, long cyclic life and low environmental pollution, and they have been extensively applied in electric vehicles (EV), hybrid electric vehicles (HEV), portable electronics and aerospace over the last few years [1–3]. Nevertheless, compared to rechargeable batteries, their relatively low energy density falls short of satisfying the ever–increasing demands for power sources [4–6]. Therefore, progressive effort has been devoted to obtaining high energy density supercapacitors, without impairing their cyclic life and power density [7–12].

One promising strategy is the preparation of faradic pseudocapacitors, which contains a capacitor-type electrode and a battery-type electrode. In the pseudocapacitors design, the capacitor-type electrode could share the high charge/discharge currents during cycling, retaining the high rate capability and long cyclic life of the supercapacitors, while the faradic electrode significantly boosts the specific capacitance of the system, providing large energy density [13]. Within the supercapacitors, electrode materials play a significant role in the performance of the electrodes, which have become an important factor for advancing the investigation of asymmetric supercapacitors. As a consequence, various transition metal oxides, conductive polymer materials, transition metal, metal sulfides and metal hydroxides have been extensively explored to improve the energy density of supercapacitors [14–18]. Among those appealing electrode materials, transition metal cobalt (Co) has attracted extensive attention due to its unique physical and chemical properties, such as good stability in the air, facile preparation and high electrochemical activity, which enable Co much potential in the utilizations of asymmetric supercapacitors [19].

However, the practical implementation of pure Co electrode is hampered by the agglomeration of the active material, stemming from its large surface energy and small size. The effect inevitably causes low specific capacitance and inferior rate capability of the electrode [19]. One efficient approach to circumvent the problems is the preparation of Co/C hybrid materials, such as Co/graphite composites, Co/graphene nanocomposites, etcetera [19–22]. For instance, Barakat et al. have prepared Cd-doped Co nanoparticles encapsulated in graphite, which have shown good stability as a supercapacitor [21]. In general, the combination of carbon and Co improves the electrochemical performance of Co electrode effectively [19–22]. However, as a promising electrode material for supercapacitors, it is highly desired to explore other variety of carbon materials to improve the electrochemical properties of Co electrode.

In this work, to expand the application of coal-based activated carbon and the extent of Co-based composites as electrode materials for supercapacitors, we therefore put forward an easy and cost-effective precipitation approach to prepare Co/coal-based activated carbon (Co/CAC) composites. Results suggest that Co nanoparticles are well dispersed on the surface of recyclable, abundant, non-toxic and easily prepared coal-based activated carbon (CAC), which restrains the agglomeration of Co nanoparticles efficiently. Compared with pure Co and bare CAC, the composites exhibit enhanced capacitance, which could be ascribed to the synergistic effect of the combination of Co nanoparticles and the coal-based activated carbon.

## 2. EXPERIMENTAL

### 2.1 Synthesis of Co/CAC composite materials

CAC was prepared by physical activation method. Firstly, coal-blending of Shan Dong Coal (SDC, 40%), Yong Cheng Coal (YCC, 40%) and Tai Xi Coal (TXC, 20%) was pulverized to powder (around 0.074 mm in diameter) and mixed adequately. Subsequently, the mixture was re-agglomerated into coal briquettes under 150 MPa and crushed into desired size (3–5 mm). The obtained briquettes

were then subjected to carbonization at 650 °C for 30 min and activation at 880 °C for 230 min with the amount of 1.0 mL H<sub>2</sub>O/(h g char) in a pipe furnace. After cooling to room temperature, the activated products were crushed to desired size to obtain CAC.

Co/CAC composites were prepared by a facile precipitation approach. Typically, 400 mg of citric acid and 40 mg of CAC was added into 50 mL of H<sub>2</sub>O, respectively, and stirred for 10 minutes under ultrasound. Subsequently, 400 mg of CoCl<sub>2</sub>·6H<sub>2</sub>O was added in the foregoing solution under ultrasonic stirring. The solution was then transferred into a 250 mL of three-neck flask, and kept for stirring in an ice-water bath. Thereafter, 50 ml of NaBH<sub>4</sub> (1600 mg) aqueous solution was added dropwise to the above solution. The mixture was tempestuously stirred for 2 h in the ice-water bath, and then filtered and washed with water and ethanol for several times. The resultant products were dried at 60 °C in vacuum. For comparison, bare Co (Co) was prepared via the same method without CAC.

## 2.2 Microstructural Characterizations

The structures and morphologies of the as-prepared samples were characterized by X-ray diffraction (XRD, Bruker D8 ADVANCE X-ray diffractometer with Cu Ka radiation), scanning electron microscopy (SEM, FEI Quanta 250 FEG equipped with energy dispersive X-ray spectroscopy (EDS)) and transmission electron microscopy (TEM, FEI Tecnai G2 F20, 200kV). The content of CAC in Co/CAC was analyzed by Vario EL cube (Elementar, Germany).

## 2.3 Electrochemical Characterizations

Electrochemical tests were carried out using a conventional three-electrode cell. The working electrode was prepared by mixing active material powders with 10 w.t.% of conductive agent (acetylene black) and 10 w.t.% of binder (polytetrafluorene ethylene). A small quantity of distilled water was added to form a homogeneous mixture, which was subsequently pressed onto the nickel foam (10 mm×10 mm) and dried at 60 °C in vacuum. A platinum foil was used as the counter electrode. An Hg/HgO electrode was acted as the reference electrode. The electrolyte solution was 6 mol L<sup>-1</sup> KOH aqueous solution. Cyclic voltammetry measurements were conducted on a CHI 604E electrochemical workstation (0.1–0.6 V *vs.* Hg/HgO). Charge/discharge tests were investigated by Neware battery testing workstation in a voltage window of 0.1–0.5 V (*vs.* Hg/HgO). Electrochemical impedance spectroscopy was recorded by CHI 604E electrochemical workstation under following conditions: AC voltage amplitude of 5 mV, frequency ranges of 10<sup>5</sup>–10<sup>-2</sup> Hz.

# 3. RESULTS AND DISCUSSION

## 3.1 Characterization of samples

The overall preparation scheme of Co/CAC is depicted in Fig. 1. It is generally known that CAC exhibits plenty of surface functional groups such as hydroxyl groups, carboxylic group et al.

[23]. The functional groups of CAC could afford anchor sites, where metal ions could be absorbed through electrostatic attraction. During the ultrasonic treatment process,  $\text{Co}^{2+}$  ions could be attached to the functional groups of CAC via electrostatic interaction. Then, the absorbed  $\text{Co}^{2+}$  ions react with added  $\text{NaBH}_4$  to transform into Co nanoparticles, which are firmly anchored on the surface of CAC.

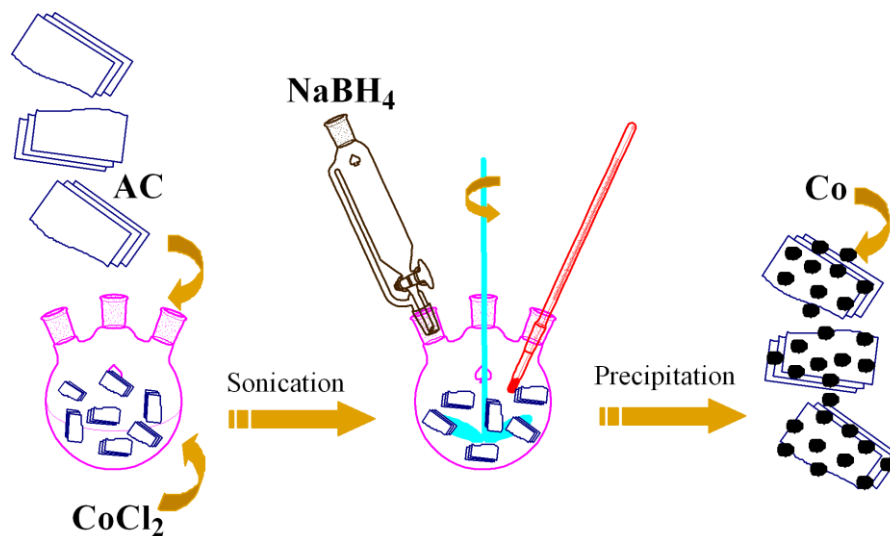


**Figure 1.** Schematic illustration for the preparation process of Co/CAC.

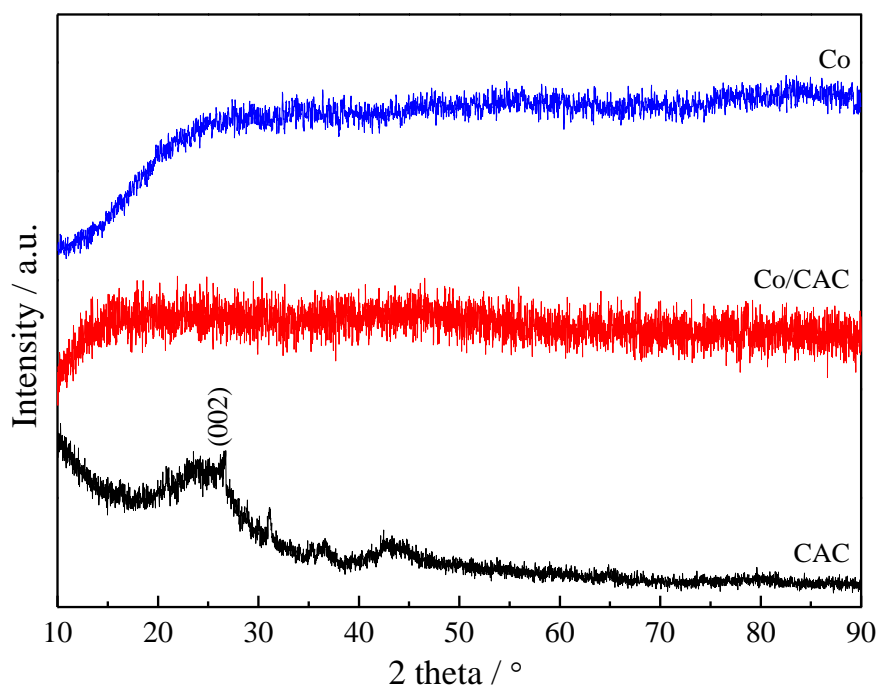


**Figure 2.** X-ray diffraction patterns of Co, CAC and Co/CAC.

The chemical compositions of CAC, Co and Co/CAC are determined by XRD, as presented in Fig. 2. The diffraction peak of CAC corresponding to (002) crystalplane of carbon is weak and broad,

which demonstrates the highly amorphous nature of CAC. It should be noted that during the preparation process,  $\text{Co}^{2+}$  was reduced to metallic Co by adding sufficient  $\text{NaBH}_4$  [24, 25]. However, no obvious diffraction peak is observed in the XRD pattern of Co, which indicates that metallic Co is in the amorphous state. Similar phenomenon has also been observed in Co/CAC composites. Meanwhile, no obvious diffraction peak assigned to CAC is observed for Co/CAC, suggesting the homogeneous coating and dispersion of cobalt particles on CAC.

The morphologies of the as-prepared materials have been investigated by SEM (Fig. 3). As shown in Fig. 3a, Co nanoparticles are aggregated with each other severely, leading to a compact structure. The SEM image of Co/CAC is displayed in Fig. 3b. It is revealed that a large number of Co nanoparticles are homogeneously dispersed on CAC, which prevents Co particles from aggregation efficiently. The elemental composition of Co/CAC is further confirmed with EDS (Fig. 3c). The EDS results displays that Co/CAC consist of Co element, C element and O element, and is in agreement with the foregoing analysis. The morphology of Co/CAC is also observed by TEM (Fig.3d). The result suggests that Co nanoparticles are discretely dispersed on the surface of CAC, and most of the particles are 150–200 nm in diameter. This unique microstructure, Co nanoparticles uniformly distributed on CAC, will be beneficial for the fast diffusion and migration of the electrolyte ions, and is anticipated to show superior electrochemical capacitance.

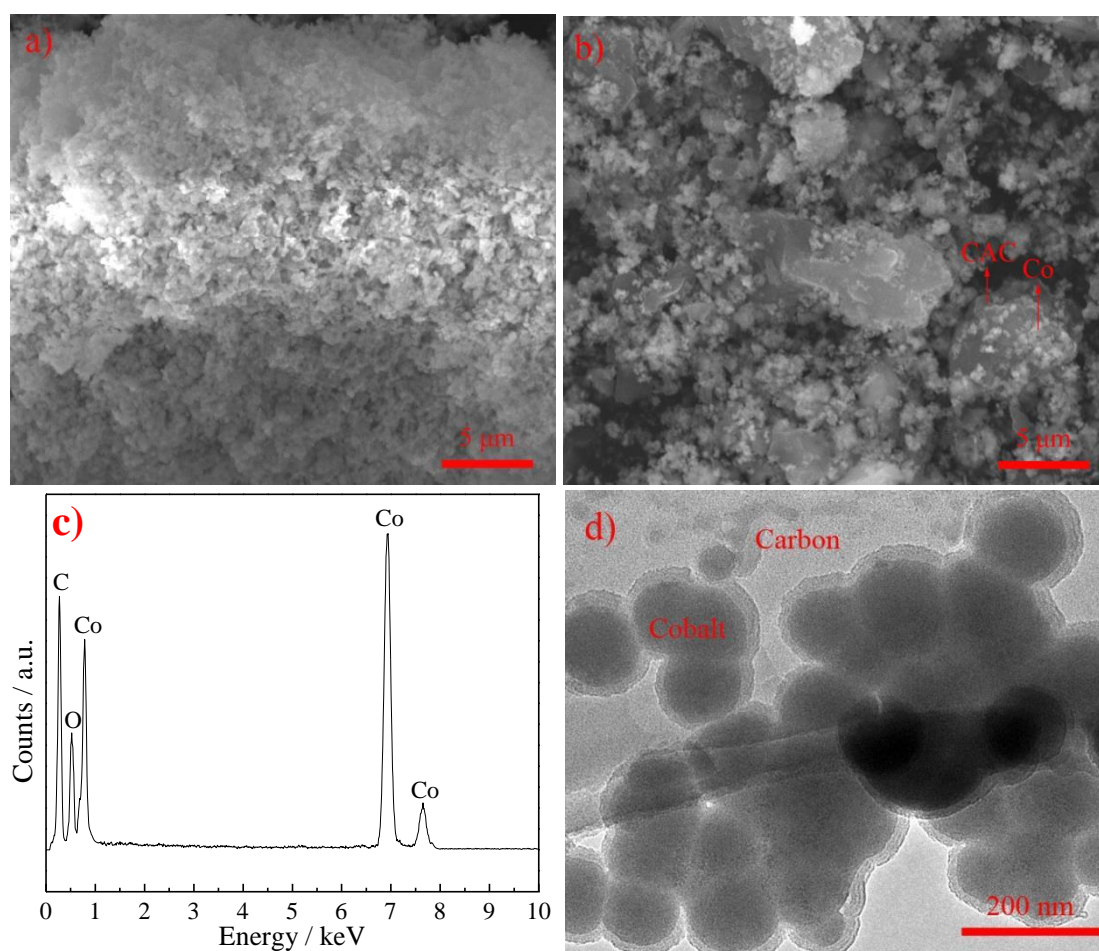


**Figure 3.** SEM images of a) Co, b) Co/CAC, c) the corresponding EDS image of b), d) TEM image of Co/CAC.

The mass percentage of CAC and Co in Co/CAC composites is analyzed by elemental analysis. The CAC% of the composites is estimated according to the mass of  $\text{CO}_2$ , deriving from burning Co/CAC. The result suggests that Co/CAC consist of 71.4 wt.% of Co and 28.6 wt.% of CAC.

### 3.2 Electrochemical properties of samples

The capacitive performances of the as-prepared samples are initially examined by cyclic voltammetry (CV) measurements. CV curves of Co, CAC and Co/CAC at a scanning rate of  $10 \text{ mV s}^{-1}$  are shown in Fig. 4. The CV curve of CAC is close to rectangle, which demonstrates its ideal capacitive performance. In contrast, both of the CV curves of Co and Co/CAC comprise a pair of redox peaks, which is related to the following faradaic redox reaction [22],  $\text{Co} + 2\text{OH}^- = \text{Co}(\text{OH})_2 + 2\text{e}^-$ . The results suggest that the Co and Co/CAC electrodes display apparent pseudo-capacitive trait, which is distinct from electric double-layer capacitance. Meanwhile, the enclosed area in the CV curve of Co is significantly smaller than that of Co/CAC at the same scanning rate, indicating that Co exhibit lower specific capacitance than Co/CAC. The foregoing CV analysis demonstrates that the well-organized microstructure of the Co/CAC composites prompts faradaic reaction of metallic Co.

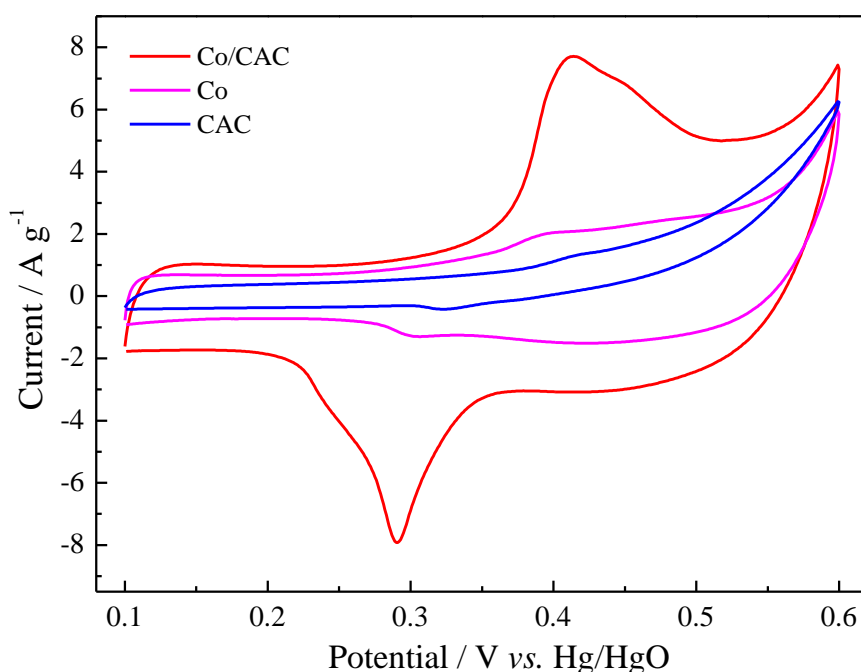


**Figure 4.** CV curves of Co, CAC and Co/CAC at a scanning rate of  $10 \text{ mV s}^{-1}$ .

The charge/discharge behaviors of Co, CAC and Co/CAC are investigated at a current density of  $2 \text{ A g}^{-1}$  in Fig. 5. The results show that the charge/discharge curves of CAC is linear and symmetrical, demonstrating an ideal capacitance characteristic of CAC. Non-linear charge/discharge curves are obtained for both the Co and Co/CAC electrodes, indicating typical features of pseudo-

capacitive materials. Meanwhile, the specific capacitance of Co is obviously increased by the introduction of CAC. On the one hand, the presence of CAC increases the contact between the electrolyte and Co nanoparticles. On the other hand, CAC could restrain the agglomeration of the active materials during the charge/discharge process.

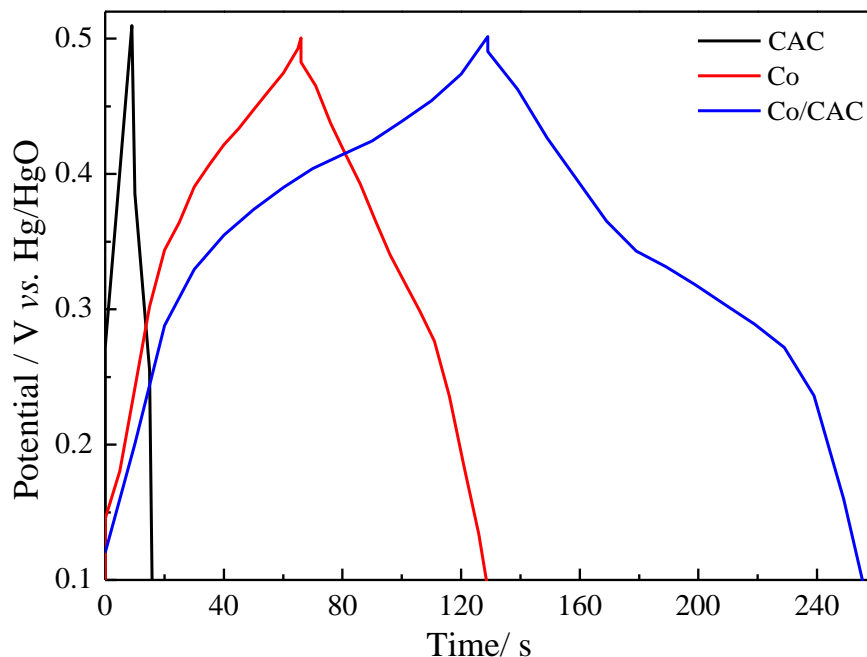


**Figure 5.** The galvanostatic charge/discharge curves of Co, CAC and Co/CAC at  $2 \text{ A g}^{-1}$ .

The comparison of the cycling performance of Co, CAC and Co/CAC is shown in Fig. 6. Intriguingly, the combination of Co and CAC enhances electrochemical properties of the whole system. Specific capacitances of the as-prepared materials are calculated according to the equation [26–28],  $C_s = I \times \Delta t / (m \times \Delta V)$ , where  $C_s$ ,  $I$ ,  $\Delta t$ ,  $m$ ,  $\Delta V$  are the specific capacitance ( $\text{F g}^{-1}$ ), the discharge current (A), the discharge time (s), the mass of active materials (g), the potential change (V), respectively. The Co/CAC composite material shows good cyclic performance with a specific capacitance of  $615 \text{ F g}^{-1}$  after 3000 cycles at  $2 \text{ A g}^{-1}$ , giving a 98% capacitance retention rate. The electrochemical performance of Co/CAC is better than many similar reports [21, 31]. Although the specific capacity is lower than some reports, the preparation process of Co/CAC is easier. Besides, Co/CAC was fabricated with CAC as the support, which is much cheaper than similar reports, and hence facilitating the practical application of the composite material [19, 20, 22]. Comparatively, bare Co and pure CAC active materials exhibit inferior capacitive performance with specific capacitances of  $300 \text{ F g}^{-1}$  and  $20 \text{ F g}^{-1}$ , respectively. The results obtained indicate that the composite material exhibits synergetic effect between Co and CAC. For one thing, Co nanoparticles are homogeneously dispersed on CAC, facilitating the penetration of the electrolyte. For the other, the introduction of CAC could prevent the agglomeration of Co particles, and hence enhancing their electrochemical utilization.

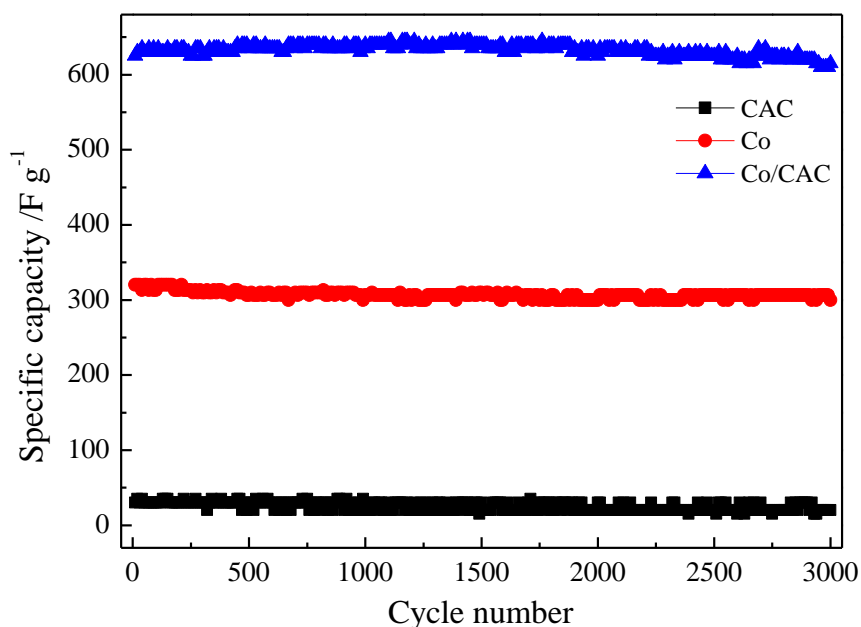


**Figure 6.** Cycling performances of Co, CAC and Co/CAC at a current density of  $2 \text{ A g}^{-1}$ .

Rate capability of Co/CAC is displayed to further investigate the capacitive performance of the composite material. Fig. 7 shows the galvanostatic charge/discharge curves of Co/CAC at various current densities. The typical shapes of the curves indicate the pseudocapacitance of the electrode, being coincident with the foregoing CV results. The specific capacitances of Co/CAC at current densities of 4, 6, 8, 10, 16, 20  $\text{A g}^{-1}$  are 540, 522, 513, 504, 504, 495  $\text{F g}^{-1}$ , respectively. The results show that the specific capacitance of Co/CAC obtained at 20  $\text{A g}^{-1}$  retains 91.7% of the value obtained at 4  $\text{A g}^{-1}$ . The rate capability of the as-prepared Co/CAC is superior to that of many similar reports [20, 21, 31], which demonstrates the impressive rate performance of the composite material.

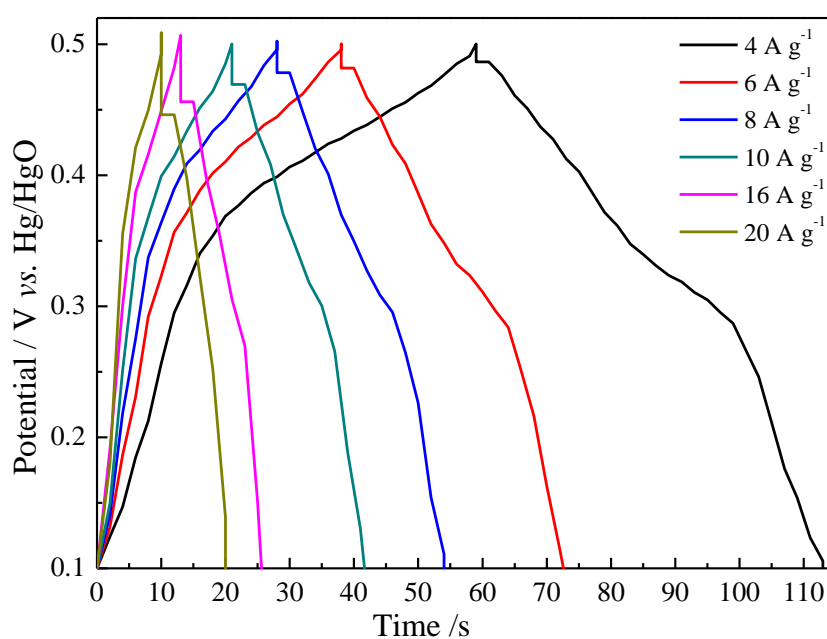


**Figure 7.** Galvanostatic charge/discharge curves of Co/CAC at different current densities.

#### 4. CONCLUSIONS

In summary, Co/CAC nanocomposites have been prepared via a facile precipitation process for supercapacitors. Specific capacitances of Co, CAC and Co/CAC are 300, 20 and 615 F g<sup>-1</sup> after 3000 cycles at 2 A g<sup>-1</sup> respectively, indicating that the combination of pseudocapacitive Co nanoparticles and CAC matrix results in synergistic performance. In addition, even at a high current density of 20 A g<sup>-1</sup>, the composite material exhibits an impressive rate capability of 495 F g<sup>-1</sup>. Importantly, EIS results demonstrate that the introduction of CAC can not only promote the penetration of the electrolyte, but also decrease the transfer resistance of the electrode.

#### ACKNOWLEDGEMENTS

This work was supported by the Fundamental Research Funds for the Central Universities (No. 2015QNA26).

#### References

1. L. Yang, H. Li, H. Liu and Y. Zhang, *Int. J. Electrochem. Sci.*, 12 (2017) 1.
2. L. Wang, D. Wang, J. Zhu and X. Liang, *Ionics*, 19 (2013) 215.
3. L. Zhu, W. Wu, Y. Zhu, W. Tang and Y. Wu, *J. Phys. Chem. C*, 119 (2015) 7069.
4. T. Yi, J. Mei, Y. Zhu and Z. Fang, *Chem. Commun.*, 51 (2015) 14050.
5. L. Wang, H. Tian, D. Wang, X. Qin and G. Shao, *Electrochim. Acta*, 151 (2015) 407.
6. J. Zhu, G. Hu and J. Zhang, *Mater. Lett.*, 185 (2016) 565.
7. H. Wang, C. Qing, J. Guo, A. Aref, D. Sun, B. Wang and Y. Tang, *J. Mater. Chem. A*, 2 (2014) 11776.
8. G. Cai, X. Wang, M. Cui, P. Darmawan, J. Wang, A. Eh and P. Lee, *Nano Energy*, 12 (2015) 258.
9. R. Ramachandran, M. Saranya, P. Kollu, B. Raghupathy, S. Jeong and A. Grace, *Electrochim. Acta*, 178 (2015) 647.
10. Z. Li, J. Han, L. Fan and R. Guo, *CrystEngComm.*, 17 (2015) 1952.
11. L. Wang, Y. Ma, M. Yang and Y. Qi, *RSC Adv.*, 5 (2015) 89069.
12. M. Javed, S. Dai, M. Wang, Y. Xi, Q. Lang, D. Guo and C. Hu, *Nanoscale*, 7 (2015) 13610.
13. G. Wang, L. Zhang and J. Zhang, *Chem. Soc. Rev.*, 41 (2012) 797.
14. F. Zhou, Q. Liu, J. Gu, W. Zhang and D. Zhang, *J. Power Sources*, 273 (2015) 945.
15. W. Zhang, L. Kong, X. Ma, Y. Luo and L. Kang, *J. Power Sources*, 269 (2014) 61.
16. R. Xing, T. Jiao, Y. Liu, K. Ma, Q. Zou, G. Ma and X. Yan, *Polymers*, 8 (2016) 181.
17. L. Cui, M. Ji, L. Mao, S. Kang, Y. Wang and H. Shi, *J. Electrochem. Soc.*, 163 (2016) A2017.
18. D. Wu, T. Xiao, X. Tan, P. Xiang, L. Jiang, Z. Kang and P. Tan, *Electrochim. Acta*, 198 (2016) 1.
19. G. Liu, L. Wang, B. Wang, T. Gao, and D. Wang, *RSC Adv.*, 5 (2015) 63553.
20. L. Wang, D. Wang, X. Hua, J. Zhu and X. Liang, *Electrochim. Acta*, 76 (2012) 282.
21. N. Barakat, A. El-Deen, G. Shin, M. Park and H. Kim, *Mater. Lett.*, 99 (2013) 168.
22. J. Balamurugan, T. Thanh, N. Kim and J. Lee, *J. Mater. Chem. A*, 4 (2016) 9555.
23. X. Xiao, D. Liu, Y. Yan, Z. Wu, Z. Wu and G. Cravotto, *J. Taiwan Inst. Chem. E.*, 53 (2015) 160.
24. B. Feng, J. Xie, G. Cao, T. Zhu and X. Zhao, *New J. Chem.*, 37 (2013) 474.
25. J. Zhu, D. Wang, T. Liu and C. Guo, *Electrochim. Acta*, 125 (2014) 347.
26. J. Yan, E. Khoo, A. Sumboja and P. Lee, *ACS Nano*, 4 (2010) 4247.
27. G. Yu, L. Hu, M. Vosgueritchian, H. Wang, X. Xie, J. McDonough, X. Cui, Y. Cui and Z. Bao, *Nano Lett.*, 11 (2011) 2905.
28. S. Bao, C. Li, C. Guo and Y. Qiao, *J. Power Sources*, 180 (2008) 676.

29. X. Chen, Y. He, H. Song and Z. Zhang, *Carbon*, 72 (2014) 410.
30. Y. Wang, C. Guo, J. Liu, T. Chen, H. Yang and C. Li, *Dalton Trans.*, 40 (2011) 6388.
31. J. Yang, C. Zeng, F. Wei, J. Jiang, K. Chen and S. Lu, *Mater. Design*, 83 (2015) 552.

© 2017 The Authors. Published by ESG ([www.electrochemsci.org](http://www.electrochemsci.org)). This article is an open access article distributed under the terms and conditions of the Creative Commons Attribution license (<http://creativecommons.org/licenses/by/4.0/>).